Int J Mater Form (2009) Vol. 2 Suppl 1:379–382
DOI 10.1007/s12289-009-0458-0

MK MODELLING OF SHEET FORMABILITY IN THE INCREMENTAL SHEET FORMING PROCESS, TAKING INTO ACCOUNT THROUGH-THICKNESS SHEAR

Philip Eyckens[1*], Jihane Del-lero Moreau[1], Joost R. Duflou[2], Albert Van Bael[1,3] and Paul Van Houtte[1]

[1] Department MTM, Faculty of Engineering, Katholieke Universiteit Leuven, Belgium.
[2] Mechanical Engineering Department, Katholieke Universiteit Leuven, Belgium.
[3] IWT, KHLim (Limburg Catholic University College), Campus Diepenbeek, Belgium.

ABSTRACT: This paper presents experimental measurements of the Through-Thickness Shear (TTS), (also known as out-of-plane shear) that occurs during Single Point Incremental Forming (SPIF) of low carbon steel into cone-shaped geometries. The measurements show the dependence of TTS on the cone wall angle. Also formability predictions are presented, using a Marciniak-Kuczyński (MK) type of forming limit model which can take TTS explicitly into account [1]. It is seen that the presence of TTS in the process delays the onset of localized necking and thus can be a contributing factor to the very high formability during SPIF that is observed.

KEYWORDS: Single Point Incremental Forming, Marciniak-Kuczyński forming limit model, through-thickness shear.

1 INTRODUCTION

Single Point Incremental Forming (SPIF) is a dieless sheet forming process that has emerged over the last decade as an economic alternative for rapid manufacturing and small batch production. The exact deformation mechanism of this process is not yet fully understood, however previous Finite Element simulations [2] show a highly non-linear deformation mechanism. Recent experimental studies [3,4] have shown the existence of Through-Thickness Shear (TTS) in this process.

In this paper, additional experimental results on TTS in SPIF are presented for a low carbon steel. The focus lies on the effect of the wall angle on the amount of TTS. These experimental measurements are used to predict localized necking based on a Marciniak-Kuczyński (MK) forming limit model that takes the TTS explicitly into account, under the assumption of monotonic deformation, and using a simple constitutive law. The results indicate, in a qualitative way, that TTS in SPIF contributes to the high formability of this process.

2 EXPERIMENT

2.1 EXPERIMENTAL SET-UP

SPIF is applied to DC01 low carbon steel sheets of initial thickness θ_0=1.15mm to form truncated cone geometries. The sheet is fully clamped to a backing plate with a circumferential orifice of radius r_b=91mm. The CNC-controlled tool, hemispherically ended with a radius r_t=5mm, is moved with a speed of 2000 mm/min along the toolpath that consists of a succession of circles with diminishing radius, alternated by a vertical step-down, as shown in Figure 1.

The rotational tool speed around the z-axis is set so that a rolling contact is established at half the theoretical contact height along the cone wall. Oil lubrication is applied to the sheet-tool contact throughout the process.

Cones with different wall angles α are made (ranging from 40° to 67°), all having a maximum inner cone radius r_c=87mm. Due to the sliding contact, so-called scallop lines are formed on the cone inside surface, a cross section of which can be seen in Figure 1(b). For all the cones, the (theoretical) width in between scallop lines ΔW is set to 0.653mm (the theoretic scallop height Δh then equals 11μm), from which the vertical step-down of the tool $\Delta z = \sin(\alpha).\Delta W$ is determined. Under these process conditions the limiting wall angle is 70°, due to sheet tearing during tool step-down.

2.2 THROUGH-THICKNESS SHEAR MEASUREMENT

Prior to forming, 6 small holes (0.4mm diameter) are drilled at a radial distance of r_h=70mm from the sheet centre and remote from any step-down. After forming, samples containing the holes are placed onto a manually controlled goniometer and visually inspected through a stereomicroscope. The intersections of the deformed

* Corresponding author: MTM, KULeuven, Kasteelpark Arenberg 44 Bus 02450, BE-3001 Heverlee, Belgium. tel (+32) 16321305. fax (+32) 16321990. Philip.Eyckens@mtm.kuleuven.be

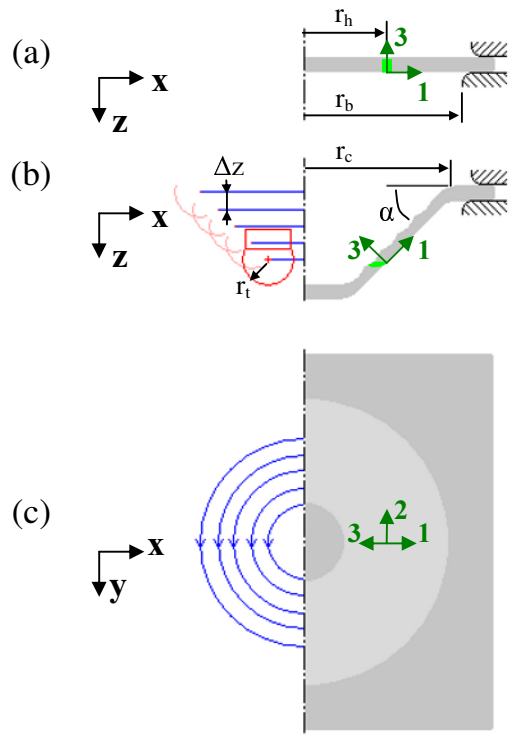

Figure 1: *Experimental set-up in the fixed x-y-z reference frame, (a) in the undeformed state, (b) and (c) in the deformed state. The contour tool path is shown in blue, the local 1-2-3 reference frame (associated with a hole) in green.*

hole and both sheet surfaces are approximately ellipses. Experience shows that the ellipse on the inner surface is generally smaller, so both can be seen simultaneously when looking from the cone outside. By tilting the sample until both ellipses are centred, two TTS-angles can be assessed. These angles γ_{13} and γ_{23} are defined in the local 1-2-3 reference frame shown in Figure 1, as the shear angles from the 3-direction (corresponding to the sheet normal) to the 1- and 2-axes, respectively. Figure 2 presents the mean values μ and standard deviations σ (sample size: 6) for each tested cone, measured by two operators.

2.3 DISCUSSION

The results, shown in Figure 2, show some trends which appear to be fairly repeatable and operator-independent.
The angle γ_{13} is generally negative, i.e. as sketched in Figure 1(b) in light green. This kind of TTS has also been observed in SPIF cones of 30° wall angle of 3mm copper plates [4], measured from a brazed grid applied to a section through the thickness of the sheet. On the other hand, in [3], the TTS-angle γ_{13} in a cone of wall angle 50° from a 1.5mm thick AA3103 sheet was found to be negligible. These observations disprove a deformation mechanism of 'pure shear' in SPIF, i.e. resulting from material displacement along the z-direction only.

The angle γ_{23}, seen in Figure 2(b), is generally positive, i.e. the cone inner surface is displaced along the tool movement direction (the local 2-direction) with respect to the cone outer surface. The same observation is made in [3,4].
From Figure 2, it can be seen that γ_{13} becomes more significant with increasing wall angle, reaching on average -28° in the 65° wall angle cone. The TTS angle γ_{23} on the other hand appears to be independent of the cone wall angle within the tested range of α, having an overall mean value of 14°.

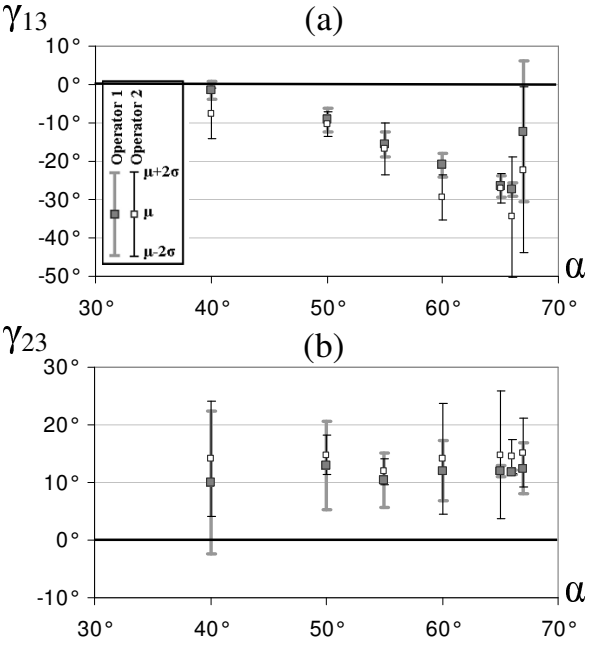

Figure 2: *Measured through-thickness shear angles: (a) γ_{13} and (b) γ_{23}, in cones with wall angle α.*

3 FORMABILITY MODELLING

A brief description of an MK model that explicitly accounts for TTS is given next. A more elaborate description of this model can be found in [1].

3.1 MK MODEL

3.1.1 Basic MK model assumptions

Metal sheets have inhomogeneous plastic properties, due to the spatial distribution of crystalline grains with different orientations, sheet thickness variations, etc… In the MK framework, the inhomogeneity is modelled as a groove with a slightly reduced initial thickness with respect to the surrounding matrix (in the current modelling, this is 99.8%). As can be seen in Figure 3, the initial groove orientation, determined by Φ_0, changes during deformation due to the matrix straining.
A monotonic deformation is imposed onto the matrix *a*, in terms of a constant velocity gradient $\mathbf{L}^a$. Through assumptions of incompressibility, force equilibrium and geometric compatibility (i.e. the following equations

(1)-(9), all 9 components of the groove velocity gradient $\mathbf{L}^b$ can be determined. They generally evolve during deformation, so an incremental procedure is applied.
For each initial groove orientation Φ_0, there is a certain major in-plane strain in the matrix, at which deformation gets localized within the groove (subsequently called the necking strain ε^*_{11}). The forming limit strain is found as the minimum of all necking strains, considering a large number of initial groove orientations Φ_0. In this paper, $-90° \le \Phi_0 \le 90°$ is considered, with steps of 1°.

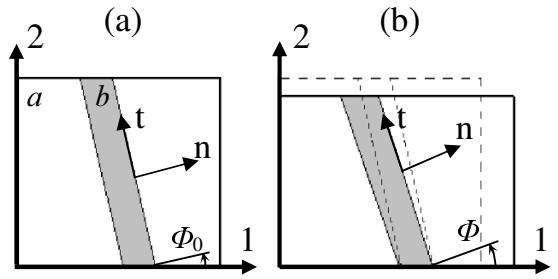

Figure 3: *MK model of (a) the undeformed and (b) a deformed state. The 1- and 2-axes denote the major and minor in-plane strain directions. The n- and t-axes are fixed to the groove b. The 3-axis (i.e. sheet thickness direction) is perpendicular to the sketched plane.*

3.1.2 Incompressibility

Incompressibility of the groove is given as:

$$L_{nn} + L_{tt} + L_{33} = 0 \tag{1}$$

3.1.3 Force equilibrium assumptions

Three components of the force along the groove-matrix interface, written in terms of stress tensor components and current thicknesses of matrix and groove θ^a and θ^b, are:

$$\theta^b \sigma^b_{nn} = \theta^a \sigma^a_{nn} \tag{2}$$

$$\theta^b \sigma^b_{tn} = \theta^a \sigma^a_{tn} \tag{3}$$

$$\theta^b \sigma^b_{3n} = \theta^a \sigma^a_{3n} \tag{4}$$

In equation (4), a non-zero matrix shear stress in the thickness direction arises from a non-zero TTS in the same plane.

3.1.4 Geometric compatibility assumptions

Five components of the groove and matrix velocity gradient (expressed in the groove reference frame), are set equal as to assure geometric compatibility:

$$L^b_{nt} = L^a_{nt} \tag{5}$$

$$L^b_{tt} = L^a_{tt} \tag{6}$$

$$L^b_{3t} = L^a_{3t} \tag{7}$$

$$L^b_{t3} = L^a_{t3} \tag{8}$$

$$L^b_{n3} = L^a_{n3} \tag{9}$$

3.1.5 Material model

For the matrix and groove material, the von Mises yield criterion is adopted in combination with a Swift hardening law determined from a uniaxial tensile test:

$$\sigma_{eq} = 515MPa\left(\varepsilon_{eq} + 0.0034\right)^{0.25} \tag{10}$$

where σ_{eq} and ε_{eq} are the von Mises equivalent stress and plastic strain, respectively.

3.2 MK MODEL APPLICATION

The MK model is applied to the deformation of the cone of 65° wall angle. The total deformation gradient **F**, expressed in the local 1-2-3 reference frame, is found to be (see also [3]):

$$\mathbf{F} = \begin{bmatrix} \theta_0/\theta & 0 & \mathrm{tg}(\gamma_{13})\theta/\theta_0 \\ 0 & 1 & \mathrm{tg}(\gamma_{23})\theta/\theta_0 \\ 0 & 0 & \theta/\theta_0 \end{bmatrix} \tag{11}$$

where θ is the final thickness and 'tg' denotes tangent. It is assumed that volume is conserved, and that there is no length change along the cone circumferential direction, i.e. the local 2-axis.
Four assumed deformation gradients **F** of the 65° wall angle cone are being used in the MK model, as shown in Table 1. Though only the last case corresponds to the actually measured total deformation, the other cases are also considered in order to illustrate the influence of TTS on the onset of localized necking.

Table 1: *Four assumed total deformations in the cone with α=65°.*

	symbol	θ/θ_0	γ_{13}	γ_{23}
1)	○	0.42	0°	0°
2)	+	0.42	-28°	0°
3)	×	0.42	0°	14°
4)	✳	0.42	-28°	14°

Earlier Finite Element investigations [2] have shown that many strain path changes take place during the SPIF. Nevertheless, it is now assumed in the MK model that the velocity gradient **L** is constant throughout the process. It can thus be calculated from (11) as:

$$\mathbf{L} = \ln(\mathbf{F})/t \tag{12}$$

in which 'ln' represents the tensorial logarithm, and t is the total time of the deformation process, which can be arbitrarily chosen for the current strain-rate insensitive material model.

3.3 MK MODEL DISCUSSION

Figure 4 presents the MK necking strain results from the different deformation gradients **F** in Table 1, for different initial groove normal directions Φ_0.

The forming limit (i.e. curve minimum) is higher for the cases that $\gamma_{23} \neq 0$. It can also be noted that $\varepsilon^*_{11}(-\Phi_0) = \varepsilon^*_{11}(\Phi_0)$, except when both TTS strains are considered (✳). Consequently, formability predictions including TTS should in general consider Φ_0 in the range [-90°;90°] and not be limited to the range [0°;90°]. Another observation is that TTS either increases the necking strain or has no effect on it, but never decreases it for the considered cases.

As developed in [1] in more detail, the delaying effect of TTS on the onset of necking, is due to a groove stress mode change towards the plane strain point on the yield locus. This mechanism is similar to the groove stress mode change found under biaxial straining without TTS. However, TTS in the n-3-plane (i.e. normal to the groove direction t) does not lead to a stress mode change in the groove. This can be seen by combining equations (2) and (4), which leads to:

$$\frac{\sigma^a_{3n}}{\sigma^a_{nn}} = \frac{\sigma^b_{3n}}{\sigma^b_{nn}} \tag{13}$$

Monotonic loading of the matrix *a* implies that the left-hand side of equation (13) is constant, from which it follows that also for the groove *b*, no stress mode change, associated with the TTS strain rate D_{3n}, is possible, and hence this kind of TTS has no effect on the necking strain.

The beneficial effect arises from the imposed TTS in the t-3-plane, which can be characterized by the absolute value of the following (normalized) strain rate:

$$|\rho_{t3}| = \left|\left(-\sin(\Phi)D_{13} + \cos(\Phi)D_{23}\right)/D_{11}\right| \tag{14}$$

Strain rate components are obtained from the symmetric part of the velocity gradient **L** in (12).

From the comparison of Figure 4(b) with 4(a), it can be seen that the higher this kind of TTS, the higher necking limits are raised compared to the deformation without TTS (○).

4 CONCLUSIONS

Experiments have shown the existence of Through-Thickness Shear (TTS) in the Single Point Incremental Forming (SPIF) process of truncated cones. The observed TTS along the cone wall direction differs from that following a pure shear mechanism in SPIF. It increases in magnitude with increasing wall angles, under the current process conditions and for the used low carbon steel DC01. On the other hand, the TTS in the circumferential direction of the cone, though non-zero, does not appear to depend significantly on the wall angle.

For the cone of 65° wall angle, the TTS measurements have been used to study the onset of localized necking, using a MK-type model recently proposed by the authors [1], which can take the effect of TTS explicitly into account. It is concluded that TTS can indeed delay the onset of localized necking in SPIF. However, a fully quantitative prediction requires a more accurate material model, accounting for anisotropic yielding and anisotropic hardening at strain path changes, as well as an accurate description of the complex deformation path in SPIF.

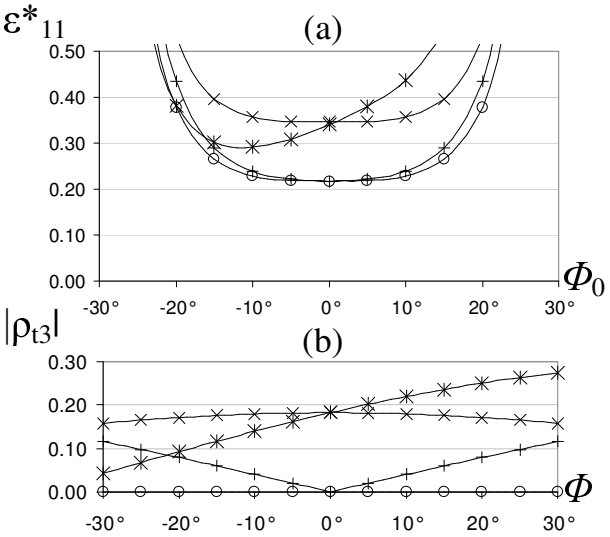

Figure 4: *Predicted necking strain ε^*_{11}, as a function of the initial groove normal direction Φ_0, and the absolute value of the imposed normalized through-thickness shear strain rate $|\rho_{t3}|$ along the t-direction, which depends on the angle Φ (cfr. equation (14)). For the symbols, see Table 1.*

ACKNOWLEDGEMENT

The authors gratefully acknowledge the financial support from the Institute for the Promotion of Innovation by Science and Technology in Flanders (IWT), from the Interuniversity Attraction Poles Program from the Belgian State through the Belgian Science Policy agency (contract IAP6/24) and from the Research Foundation Flanders.

REFERENCES

[1] Eyckens P., Van Bael A., Van Houtte P.: Marciniak-Kuczynski type modelling of the effect of through-thickness shear on the forming limits of sheet metal. *Int J Plasticity*, accepted for publication, 2008.

[2] Eyckens, P., He, S., Van Bael, A., Duflou, J., Van Houtte, P.: Finite Element Based Formability Predictions of Sheets Subjected to the Incremental Forming Process. In: *9th ComPlas Conference on Computational Plasticity*, 529-532, 2007.

[3] Eyckens, P., Van Bael, A., Van Houtte, P.: An Extended Marciniak-Kuczynski Forming Limit Model to Assess the Influence of Through-Thickness Shear on Formability. In: *7th NumiSheet Conference on Numerical Simulation of 3D Sheet Metal Forming Processes*, 193-198, 2008.

[4] Jackson, K., Allwood, J.: The Mechanics of Incremental Sheet Forming. *J Mat Proc Tech*, in Press.